

Title: Phenology and diversity in Zambia

Authors: Godlee J. L.<sup>1</sup>, Ryan C. M.<sup>1</sup>, Siampale A.<sup>2</sup>, Dexter K. G.<sup>1,3</sup>

<sup>1</sup>School of GeoSciences, University of Edinburgh, Edinburgh, United Kingdom

<sup>2</sup>Forestry Department Headquarters - Ministry of Lands and Natural Resources, Cairo Road, Lusaka, Zambia

<sup>3</sup>Royal Botanic Garden Edinburgh, Edinburgh, EH3 5LR, United Kingdom

Corresponding author:

John L. Godlee

johngodlee@gmail.com

School of GeoSciences, University of Edinburgh, Edinburgh, United Kingdom

## **Acknowledgements**

## **Author contribution statement**

JLG conceived the study, conducted the analysis, and wrote the first draft of the manuscript. AS coordinated plot data collection in Zambia, and initial data management. All authors contributed to manuscript revisions.

## **Data accessibility statement**

The data used in this study are held by the Zambian Integrated Land Use Assessment Project (ILUA-II), and were cleaned by the SEOSAW project (Socio-ecological Observatory for Southern African Woodlands). The data are not publicly available at the time of submission due to privacy concerns surrounding plot location, but can be requested from the corresponding author. An anonymised version will be made available in a data repository following review.

3 **Abstract**

4 **1 Introduction**

5 The seasonal timing and duration of tree leaf production (land-surface phenology) in dry deciduous  
6 savannas directly influences ecosystem processes. Leaf Area Index (LAI), the leaf area per unit  
7 ground area, and the green-ness of leaves are both tightly coupled with photosynthetic activity  
8 and therefore Gross Primary Productivity (GPP) (Gu et al., 2003; Penuelas, Rutishauser, and  
9 Filella, 2009). Directional shifts in GPP influence the accumulation rate of woody biomass, and  
10 affect the delicate balance between tree and grass co-occurrence in these ecosystems (Stevens et al.,  
11 2016), with potential consequences for transition between closed-canopy forest and open savanna.  
12 From a conservation perspective, within deciduous savannas, those with a longer growth period  
13 support a greater diversity and abundance of wildlife, particularly bird species but also browsing  
14 mammals (Cole, Long, et al., 2015; Araujo et al., 2017; Morellato et al., 2016; Ogutu, Piepho,  
15 and Dublin, 2013). Extreme weather patterns as a result of climate change are leading to shorter  
16 but more intense leaf production cycles in these ecosystems which are already close to the edge of  
17 their climatic envelope, with severe negative consequences anticipated for biodiversity (Bale et al.,  
18 2002). Understanding the determinants of seasonal patterns of tree leaf production in dry deciduous  
19 savannas can provide valuable information on spatial variation in vulnerability to climate change,  
20 and help to model their contribution to land surface carbon cycle models under climate change.

21 Previous studies have shown that diurnal temperature variation and precipitation are the primary  
22 determinants of tree phenological activity in water-limited savannas. At regional spatial scales,  
23 savanna phenological activity can be predicted using only climatic factors and light environment  
24 (Adole, Jadunandan Dash, and Peter M. Atkinson, 2018b), but local variation exists in leaf pro-  
25 duction cycles which cannot be attributed solely to abiotic environment. It has been repeatedly  
26 suggested that information on biotic environment play a larger role in predicting land-surface phe-  
27 nology (Adole, Jadunandan Dash, and Peter M. Atkinson, 2018a; Jeganathan, J. Dash, and P. M.  
28 Atkinson, 2014; Fuller, 1999), but implementation is most often limited to coarse ecoregions or  
29 functional vegetation types, which lack the fine-scale resolution which can take advantage of state-  
30 of-the-art earth observation data ().

31 Tree species vary in their life history strategy with regards to the timing of leaf production (Fenner,  
32 1998; Cole and Sheldon, 2017; Medina and Francisco, 1994). More conservative species (i.e. slower

growing, robust leaves, denser wood) tend to initiate leaf production (green-up) before rainfall has commenced, and persist after the rainy season has finished, despite having lower cumulative GPP during the growing season, while more resource acquisitive species and juvenile individuals tend to green-up during the rainy season, and create a dense leaf-flush during the mid-season peak of growth (). It has been suggested that this variation in leaf phenological activity between species is one aspect by which increased tree species richness causes an increase in ecosystem-level productivity in deciduous savannas (). It has also been suggested that species richness could buffer ecosystem phenology against climate warming effects (Parmesan, 2007). Building on research linking biodiversity and ecosystem function, one might expect that an ecosystem with a greater diversity of tree species might be better able to maintain consistent leaf coverage for a longer period over the year, as species vary in their optimal growing conditions due to niche complementarity, whereby coexisting species vary in their occupation of niche space due to competitive exclusion ().

In the water-limited savannas such as those found in large areas of southern Africa (), the ability of conservative tree species to maintain consistent leaf coverage in the upper canopy strata over the growing season, but particularly at the start and end of the growing season, may provide facilitative effects to other tree species and juveniles occupying lower canopy strata that are less well-adapted to moisture-limiting conditions, but are more productive, by providing shade and influencing below ground water availability through hydraulic lift ().

Variation in tree species composition, as well as species richness, is also expected to have an effect on savanna phenology in southern Africa. Savannas of a number of different types (species composition and structure) are found across southern Africa, but these are often poorly differentiated in regional-scale phenological studies () resulting in a dearth of information on the phenological behaviour of different woodland types. As our ability to remotely sense tree species composition improves, it allows us to create more tailored models of the carbon cycle which incorporate not only climatic factors, but also biotic factors which govern productivity. We therefore need to understand how species composition and biodiversity metrics affect land-surface phenology.

In the deciduous woodlands of Zambia, a highly pronounced single wet-dry season annual oscillation is observed across the majority of land area, with local exceptions in some mountainous areas (). Variation in leaf phenological activity across the country has a large influence on annual gross primary productivity. Using Zambia as a case study, we can expect similar response from deciduous woodlands across southern Africa, with important consequences for the global carbon cycle ().

While cumulative leaf production across the growing season may be the most important aspect of leaf phenology for GPP, other phenological metrics may be more important for ecosystem function and habitat provision for wildlife. Periods of green-up and senescence which bookend the growing season are key times for invertebrate reproduction (), soil biotic activity () and herbivore brows-

ing activity (). Pre-rainy season green-up in water-limited savannas provides a valuable source of moisture and nutrients before the rainy season, and can moderate the understorey microclimate, increasing humidity, reducing UV exposure, and moderating diurnal oscillations in temperature, reducing ecophysiological stress which can lead to mortality during the dry season. An increase in the time between leading tree growth and the onset of seasonal rains provides a buffer to stressful dry season climatic conditions and wildlife activity. A slower rate of green-up caused by tree species greening at different times provides an extended period of bud-burst, thus maintaining the important food source of nutrient rich young leaves for longer ().

In this study we contend that, across Zambian deciduous savannas, tree species diversity and composition influence three key measurable aspects of the tree phenological cycle: (1) the rates of greening and senescence at the start and end of the seasonal growth phase, (2) the overall length of the growth period, and (3) the lag time between green-up/senescence and the start/end of the rainy season. It is hypothesised that: (H<sub>1</sub>) due to variation among species in minimum viable water availability for growth, plots with greater tree species richness will exhibit slower rates of greening and senescence as different species green-up and senesce at different times. We expect that: (H<sub>2</sub>) in plots with greater species richness the start of the growing season will occur earlier in respect to the onset of rain due to an increased likelihood of containing a species which can green-up early, facilitating other species to initiate the growing season. We hypothesise that: (H<sub>3</sub>) plots with greater species richness will exhibit a longer growth period and greater cumulative green-ness over the course of the growth period, due to a higher resilience to variation in water availability, acting as a buffer to ecosystem-level productivity. Finally, we hypothesise that: (H<sub>4</sub>) irrespective of species diversity, variation in tree species composition and vegetation type will cause ecologically important variation in the phenological metrics outlined above.

## 2 Materials and methods

### 2.1 Data collection

We used plot-level data on tree species diversity across 705 sites from the Zambian Integrated Land Use Assessment Phase II (ILUA-II), conducted in 2014 (Mukosha and Siampale, 2009; Pelletier et al., 2018). Each site consisted of four 20x50 m (0.2 ha) plots positioned in a square around a central point, with a distance of 500 m between each plot (Figure 2). The original census contained 993 sites, which was filtered in order to define study bounds and to ensure data quality. Only sites with  $\geq 50$  stems ha<sup>-1</sup>  $\geq 10$  cm DBH (Diameter at Breast Height) were included in the analysis, to ensure all sites represented woody savanna rather than ‘grassy savanna’, which is considered a separate biome with very different species composition and ecosystem processes governing phenology (Parr

et al., 2014). Sites in Mopane woodland were removed by filtering sites with greater than 50% of individuals belonging to *Colophospermum mopane*, preserving only plots with Zambesian tree savanna/woodland. Plots dominated by non-native tree species ( $\geq 50\%$  of individuals), e.g. *Pinus* spp. and *Eucalyptus* spp. were also excluded, as these species may exhibit non-seasonal patterns of leaf production ().

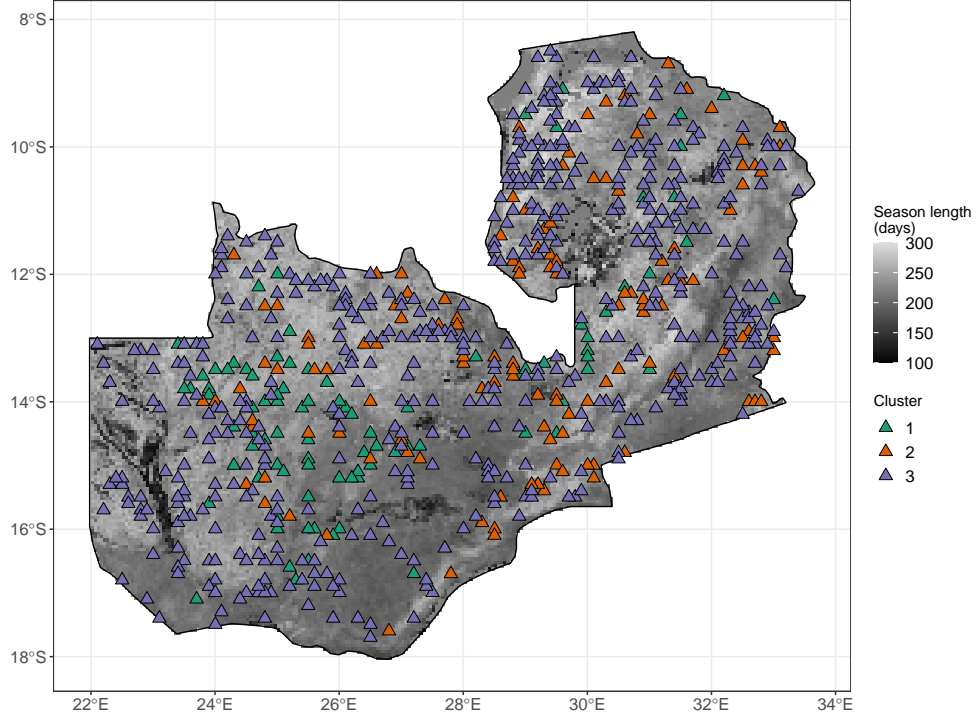


Figure 1: Distribution of study sites within Zambia as triangles, each consisting of four plots. Sites are coloured according to vegetation compositional cluster as identified by Ward’s clustering algorithm on euclidean distance of plots in the first two axes of NSCA ordination space. Zambia is shaded according to growing season length as estimated by the MODIS VIPPHEN-EVI2 product, at 0.05°spatial resolution (Didan and Barreto, 2016).

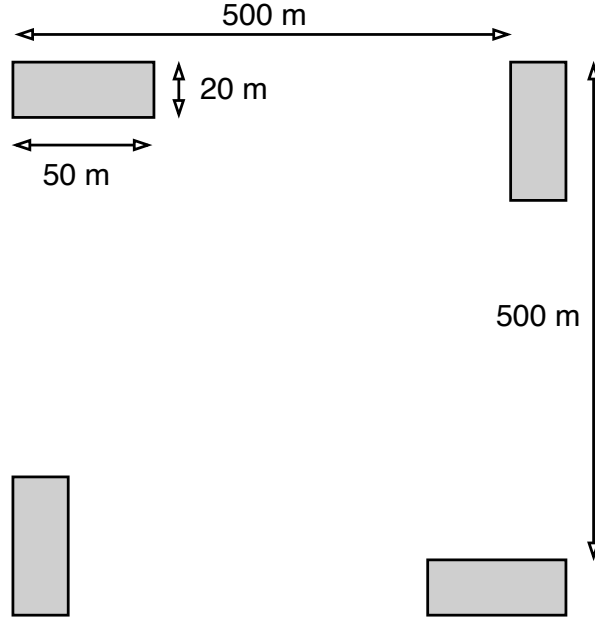


Figure 2: Schematic diagram of plot layout within a site. Each 20x50 m (0.2 ha) plot is shaded grey. The site centre is denoted by a circle. Note that the plot dimensions are not to scale.

Within each plot, the species of all trees with at least one stem  $\geq 10$  cm DBH were recorded. Plot data was aggregated to the site level for analyses to avoid pseudo-replication caused by the more spatially coarse phenology data. Tree species composition varied little among the four plots within a site, and were treated as representative of the woodland in the local area. Using the Bray-Curtis dissimilarity index of species abundance data, we calculated that the mean pairwise compositional distance between plots within a site was lower than the mean compositional distance across all pairs of plots in 88.4% of cases.

To quantify phenology at each site, we used the MODIS MOD13Q1 satellite data product at 250 m resolution (Didan, 2015). The MOD13Q1 product provides an Enhanced Vegetation Index (EVI) time series at 16 day intervals. EVI is widely used as a measure of vegetation growth, as an improvement to NDVI (Normalised Differential Vegetation Index), which tends to saturate at higher values. Annual cumulative EVI is well-correlated with gross primary productivity and so can act as a suitable proxy (). We used all scenes from January 2015 to January 2021 with less than 20% cloud cover covering the study area. All sites were determined to have a single annual growth season according to the MODIS VIPPHEN product (), which assigns pixels ( $0.05^\circ$ , 5.55 km at equator) up to three growth seasons per year. We stacked yearly data between 2015 and 2020 and fit a General Additive Model (GAM) to produce an average EVI curve. We estimated the start and end of the growing season using first derivatives of the GAM. Start of the growing season was identified as the first day where the model slope exceeds half of the maximum positive model slope for a continuous period of 20 or more days, following White et al. (2009). Similarly, we defined the end of

126 the growing season as the final day of the latest 20 period where the GAM slope meets or exceeds  
 127 half of the maximum negative slope. We estimated the length of the growing season as the number  
 128 of days between the start and end of the growing season. We estimated the green-up rate as the  
 129 slope of a linear model across EVI values between the start of the growing season and the point at  
 130 which the slope of reduces below half of the maximum positive slope. Similarly the senescence rate  
 131 was estimated as the slope of a linear model between the latest point where the slope of decrease  
 132 fell below half of the maximum negative slope and the end of the growing season Figure 3. We  
 133 validated our calculations of cumulative EVI, mean annual EVI, growing season length, season start  
 134 date, season end date, green-up rate and senescence rate with calculations made by the MODIS  
 135 VIPPHEN product with linear models comparing the two datasets across our study sites (Figure S1,  
 136 Table S1). We chose not to use the MODIS VIPPHEN product directly due to its more coarse  
 137 spatial resolution ( $0.05^\circ$ , 5.55 km at equator). Sites where our calculation of a phenological metric  
 138 was drastically different to the MODIS VIPPHEN estimate were excluded, under the assumption  
 139 that our algorithm had failed to capture the true value or some site specific factor precluded precise  
 140 estimation. This removed 8 sites.

141 Precipitation data was gathered using the “GPM IMERG Final Precipitation L3 1 day V06” dataset,  
 142 which has a pixel size of  $0.1^\circ$  (11.1 km at the equator) (Huffman et al., 2015), between 2015 and 2020.  
 143 Daily total precipitation was separated into two periods: precipitation during the growing season  
 144 (growing season precipitation), and precipitation in the 90 day period before the onset of the growing  
 145 season (dry season precipitation). Rainy season limits were defined as for the EVI data, using the  
 146 first derivative of a GAM to create a curve for each site using stacked yearly precipitation data,  
 147 from which we estimated the half-max positive and negative slope to identify where the GAM model  
 148 exceeded these slope thresholds for a consistent period of 20 days or more. Mean diurnal temperature  
 149 range (Diurnal  $\delta T$ ) was calculated as the mean of monthly temperature range from the WorldClim  
 150 database, using the BioClim variables, with a pixel size of 30 arc seconds (926 m at the equator)  
 151 (Fick and Hijmans, 2017). averaged across all years of available data (1970-2000).

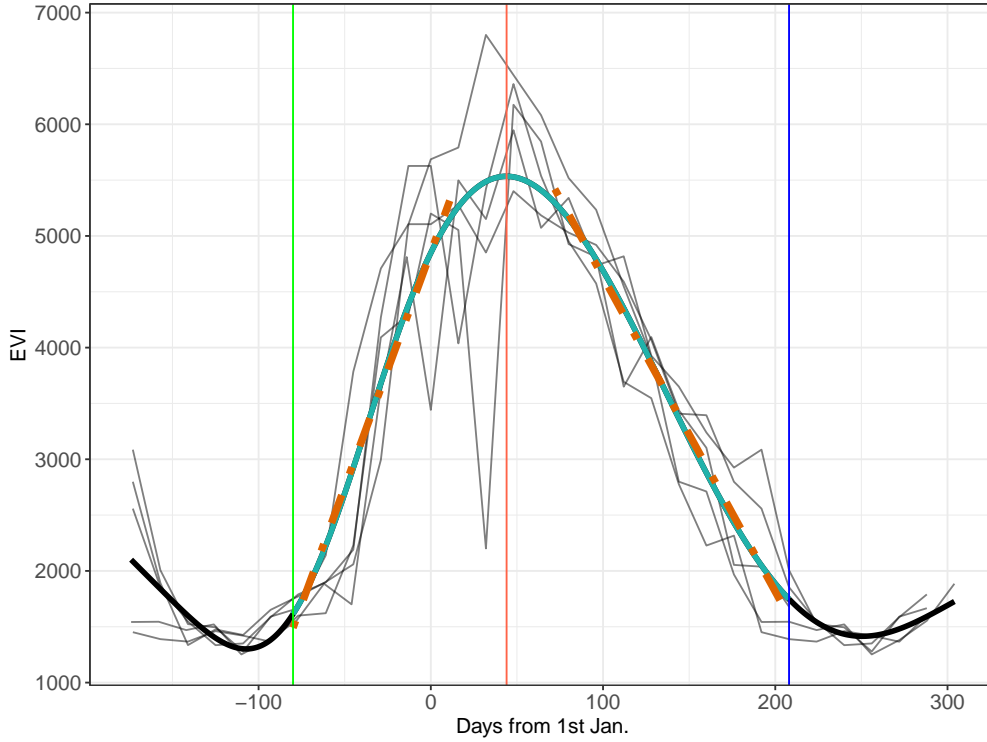


Figure 3: Example EVI time series, demonstrating the metrics derived from it. Thin black lines show the raw EVI time series, with one line for each annual growth season. The thick black line shows the GAM fit. The thin blue lines show the minima which bound the growing season. The red line shows the maximum EVI value reached within the growing season. The shaded cyan area of the GAM fit shows the growing season, as defined by the first derivative of the GAM curve. The two orange dashed lines are linear regressions predicting the green-up rate and senescence rate at the start and end of the growing season, respectively. Note that while the raw EVI time series fluctuate greatly around the middle of the growing season, mostly due to cloud cover, the GAM fit effectively smooths this variation to estimate the average EVI during the mid-season period.

## 2.2 Data analysis

To measure variation in tree species composition we used a combination of Non-symmetric Correspondence Analysis (NSCA) and agglomerative hierarchical clustering on species basal area weighted data (Kreft and Jetz, 2010; Fayolle et al., 2014). NSCA was performed using the `ade4` R package (Dray and Dufour, 2007). Scree plot analysis demonstrated that 2 axes was optimal to describe our data. These axes accounted for 17.9% of the variance in species composition according to eigenvalue decay. To guard against sensitivity to rare individuals, which can preclude meaningful cluster delineation across such a large species compositional range, we restricted the NSCA to species with five or more records, and to sites with more than five species (). We used Ward's algorithm to define clusters (Murtagh and Pierre Legendre, 2014), based on the euclidean distance of sites in



NSCA ordination space. We determined the optimal number of clusters by maximising the mean silhouette width among clusters (Rousseeuw, 1987) Figure S3. Vegetation type clusters were used later as interaction terms in linear models. We described the vegetation types represented by each of the clusters using a Dufrene-Legendre indicator species analysis (Dufrêne and P. Legendre, 1997). To describe the species diversity of each site, we calculated the Shannon-Wiener index ( $H'$ ) from species basal area rather than individual abundance, as a measure of species richness effectively weighted by a species' contribution to canopy occupancy ().  $H'$  was then transformed to the first order numbers-equivalent ( ${}^1D$ ) of  $H'$ , calculated as  $e^{H'}$  (). We use  ${}^1D$  as the primary measure of species richness in our statistical models and is subsequently referred to as such. Additionally, we calculated a separate measure of abundance evenness, using the Shannon Equitability index ( $E_{H'}$ ) (Smith and Wilson, 1996).  $E_{H'}$  was calculated as the ratio of basal area Shannon-Wiener diversity index to the natural log of total basal area per site.

We specified multivariate linear models to assess the role of tree species diversity on each of the chosen phenological metrics. We defined a maximal model structure including richness, abundance evenness, the interaction of richness and vegetation type, and climatic variables shown by previous studies to strongly influence phenology. The quality of the maximal model was compared to models with different subsets of independent variables using the model log likelihood, AIC (Akaike Information Criteria), BIC (Bayesian Information Criteria), and adjusted  $R^2$  values for each model. For each phenological metric, the best model according to the model quality statistics is reported in the results. Where two similar models were within 2 AIC points of each other, the model with fewer terms was chosen as the best model, to maximise model parsimony. All models were fitted using Maximum Likelihood (ML) to allow comparison of models (). The best model was subsequently re-fitted using Restricted Maximum Likelihood for model effect estimation (REML). Independent variables in each model were transformed to achieve normality where necessary and standardised to Z-scores prior to modelling to allow comparison of slope coefficients within a given model.

We used the **ggeffects** package to estimate the marginal means of the interaction effect of species diversity and vegetation type, to investigate vegetation type specific effects on each phenological metric (Lüdtke, 2018). Estimated marginal means entails generating model predictions across values of a focal variable, in this case species diversity, while holding non-focal variables constant. All statistical analyses were conducted in R version 4.0.2 (R Core Team, 2020).

### 3 Results

Model selection showed that richness and evenness are important determinants of each of the chosen phenological metrics, across vegetation types. The effect of richness featured and was significant in

all best models except for senescence lag and senescence rate. Evenness was a significant effect in models for cumulative EVI, season length and senescence lag only Figure 4.

3 vegetation type clusters were identified during hierarchical clustering. Cluster 3, which contains the most sites (487), consists of small stature Zambesian woodlands, as referenced by Dinerstein et al. (2017) and Chidumayo (2001), and is not dominated by a particular large canopy tree species. It is possible that these woodlands represent highly disturbed woodlands where large trees may have been removed by humans. Abundance evenness is high across sites in Cluster 3. Cluster 2 is dominated heavily by *Brachystegia boehmii*, while Cluster 1 is dominated by *Julbernardia paniculata*, both large canopy-forming trees. These two clusters likely represent variation among miombo woodland types in dominant canopy tree species. Both Clusters 1 and 2 have a similar composition of non-dominant smaller shrubby species, such as *Pseudolachnostylis maprouneifolia* (Table 1).

As expected ( $H_3$ ), richness and wet season precipitation both had positive significant effects on cumulative EVI and season length. In contrast, abundance evenness, the other aspect of tree species diversity in our models, had a significant negative effect on both cumulative EVI and season length (Figure 4).

Species richness caused a significant increase in the lag time between date of green-up and date of rainy season onset ( $H_2$ ). This effect was comparable to the effects of pre-season precipitation and diurnal temperature range, which also caused an increase in green-up lag. In contrast, senescence lag was poorly defined by our models, suggesting that some unmeasured factor remains the key driver of this phenological metric. The effects of diurnal  $\delta T$  and abundance evenness had wide confidence interval. The best model explained only 1% of the variance in senescence lag, though was still better quality than a climate-only model.

All best models including tree species diversity variables were of better quality than models which included only climatic variables Table 2. The phenological metrics best predicted were green-up lag and cumulative EVI, where models explained 26% and 34% of the variance in these variables, respectively. Senescence rate and senescence lag were the least well predicted phenological metrics, with the best model explaining 3% and 2% of their variance, respectively.

While species richness had a significant negative effect on green-up rate, as predicted by  $H_1$ , the best model, which also included pre green-up precipitation and diurnal temperature range, only explained 10% of the variance in this metric.

The slope of the relationship between species richness and phenological metrics varied among vegetation types, but maintained the same direction in all cases except rates of green-up and senescence Figure 5. Across all models however, none of the vegetation types were significantly different, according to post-hoc Tukeys's tests on marginal effects (Table S8). Clusters were largely similar in

229 their density distribution of the six phenological metrics Figure 7. The most striking differences  
230 are the presence of some sites in Cluster 3 with particularly high green-up rates. The hierarchical  
231 clustering analysis demonstrated that there was little spatial structure to the vegetation clusters  
232 identified. The key emergent trend was that Cluster 2 was absent from the southwest of the country  
233 (Figure 1) possibly due to the low levels of precipitation in this region, which could preclude many  
234 miombo tree species.

Cluster	N sites	Richness	MAP	Diurnal $\delta T$	Species	Indicator value
1	91	13(6)	966(139.7)	14(1.3)	<i>Julbernardia paniculata</i>	0.712
					<i>Psuedolachnostylis maprouneifolia</i>	0.222
					<i>Pericopsis angolensis</i>	0.209
2	127	16(6)	1054(162.5)	13(1.5)	<i>Brachystegia boehmii</i>	0.764
					<i>Psuedolachnostylis maprouneifolia</i>	0.234
					<i>Uapaca kirkiana</i>	0.227
3	487	15(7)	1037(195.9)	14(1.6)	<i>Pterocarpus angolensis</i>	0.333
					<i>Brachystegia spiciformis</i>	0.318
					<i>Diplorhynchus condylocarpon</i>	0.298

Table 1: Climatic information and Dufrene-Legendre indicator species analysis for the vegetation type clusters identified by the PAM algorithm, based on basal area weighted species abundances. The three species per cluster with the highest indicator values are shown along with other key statistics for each cluster. MAP (Mean Annual Precipitation) and Diurnal  $\delta T$  are reported as the mean and 1 standard deviation in parentheses. Species richness is reported as the median and the interquartile range in parentheses.

Response	$\delta AIC$	$\delta BIC$	$R^2_{adj}$	$\delta \log Lik$
Cumulative EVI	33.6	24.4	0.34	-18.78
Season length	16.9	12.3	0.16	-9.43
Green-up rate	8.2	3.6	0.10	-5.08
Senescence rate	-0.7	-9.8	0.02	-1.65
Green-up lag	24.6	20.1	0.21	-13.32
Senescence lag	7.7	7.7	0.02	-3.85

Table 2: Model fit statistics for each phenological metric.

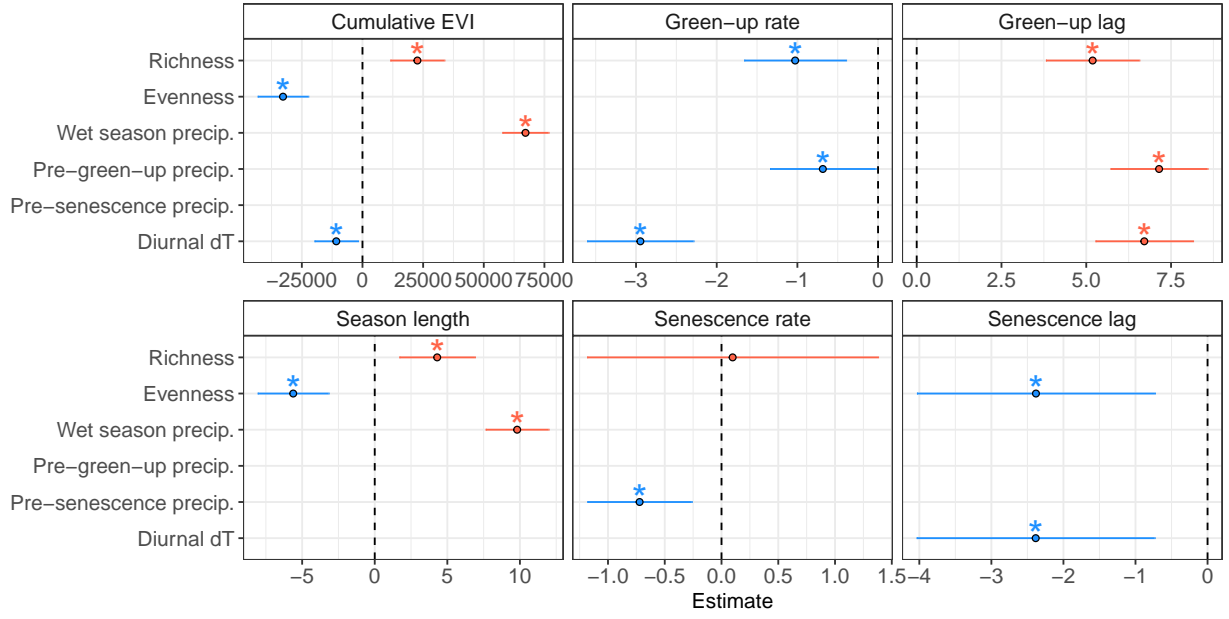


Figure 4: Standardized slope coefficients for each best model of a phenological metric. Slope estimates are  $\pm 1$  standard error. Slope estimates where the interval (standard error) does not overlap zero are considered to be significant effects.

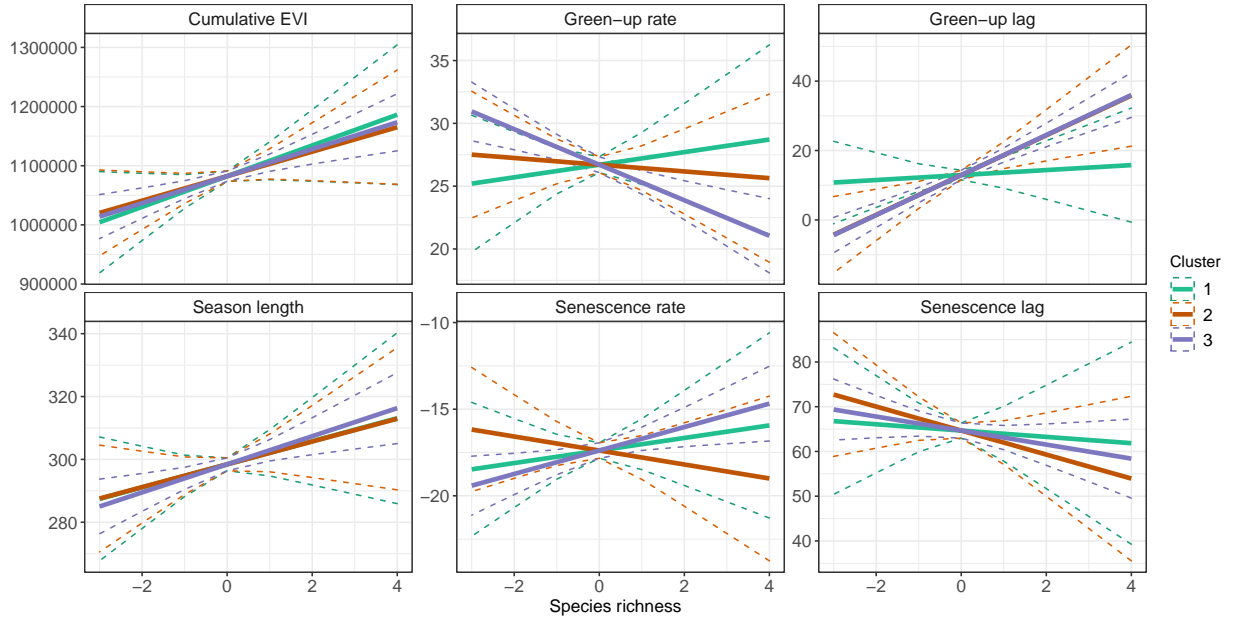


Figure 5: Marginal effects of tree species richness on each of the phenological metrics, for each vegetation type, using the best model including the interaction of species richness and vegetation cluster, for each phenological metric.

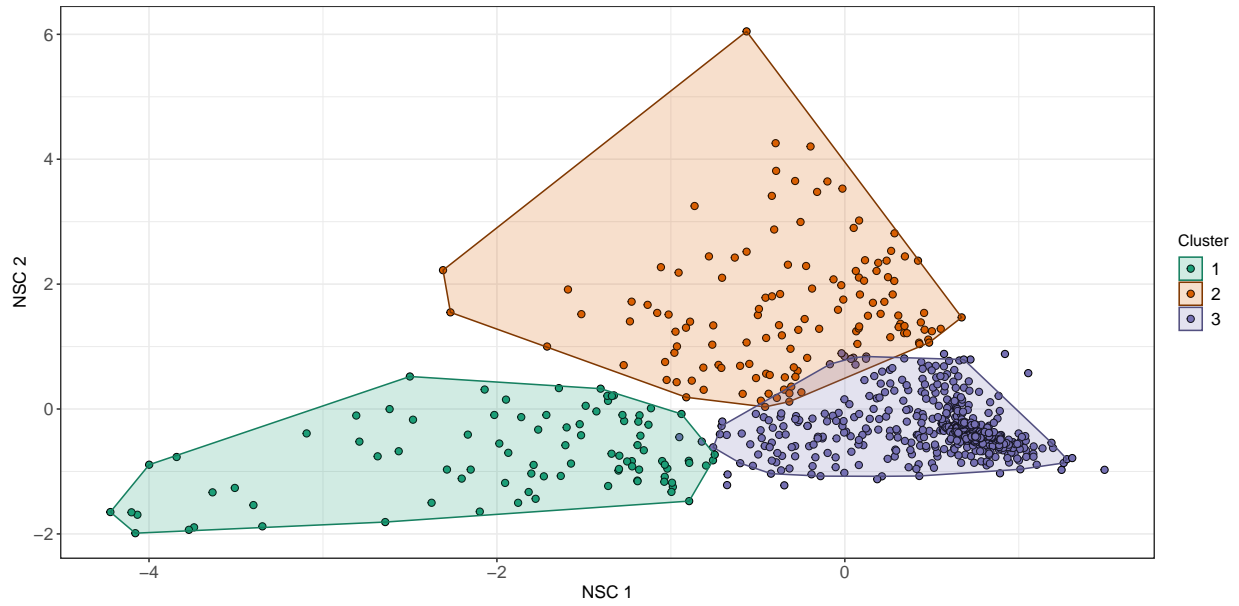


Figure 6: Plot scores of the (A) first and second, and (B) third and fourth axes of the Non-Symmetric Correspondence Analysis of tree species composition. Points are coloured according to clusters defined by Ward's algorithm on euclidean distances of the NSCA ordination axes, along with a convex hull encompassing 95% of the points in each cluster.

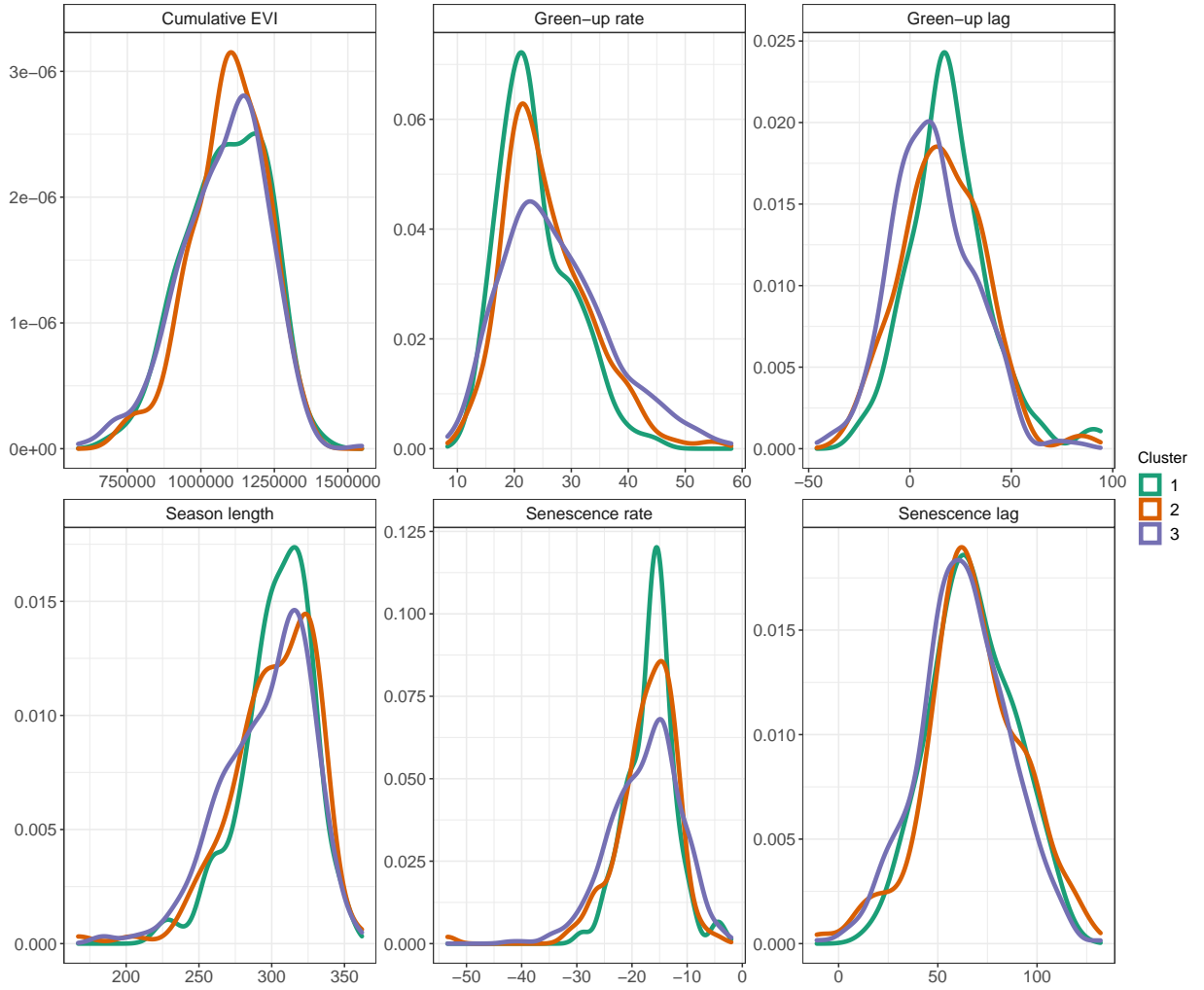


Figure 7: Density distribution of the six phenological metrics used in the study, grouped by vegetation type cluster. For a pairwise comparison of phenological metrics and their correlations, see Figure S2 and ??.

## 4 Discussion

In this study we have demonstrated a clear and measurable effect of tree species richness across various aspects of land-surface phenology in Zambian deciduous savannas. We showed that tree species richness led to an increase in cumulative EVI and season length. Additionally, species richness led to a slower rate of greening and caused the onset of greening to occur earlier with respect to the start of the rainy season. Our study lends support for a positive biodiversity - ecosystem function relationship in our chosen study area, operating through its influence on phenology. Our results exemplify the key role of tree species biodiversity in driving key ecosystem processes, which affect ecosystem structure, the wildlife provisioning role, and the gross primary productivity of ecosystems. Our finding that species richness strongly affects patterns of land-surface phenology in deciduous

245 savannas has important consequences for two pertinent fields of ecological research. Firstly, it should  
246 prompt conservation scientists to take advantage of remotely sensed land-surface phenology data to  
247 improve estimates of tree species diversity. The technology behind remote-sensing of tree species  
248 diversity is maturing fast, providing a means to rapidly and accurately assess the conservation  
249 priority of biodiversity hotspots, and to identify regions suffering biodiversity loss. Secondly, it  
250 can provide earth surface system modellers with a means to better understand how future changes  
251 in species diversity and composition will affect land-surface phenology and therefore the carbon  
252 cycle. Incorporating predictions of biotic change into carbon models has been slow, owing to large  
253 uncertainties in the effects of diversity on Gross Primary Productivity (GPP). Our study provides a  
254 link by demonstrating a strong positive relationship between species richness and EVI, which itself  
255 drives GPP.

256 Patterns of senescence were poorly predicted by species richness and evenness in our models. Cho,  
257 Ramoelo, and Dziba (2017) found that tree cover, measured by MODIS LAI data, had a significant  
258 effect on senescence rates in savannas in South Africa, which have similar climatic conditions to the  
259 sites in our study. Other studies both global and within southern African savannas have largely  
260 ignored patterns of senescence, instead focussing patterns of green-up (**Gallinat2015**). Most com-  
261 monly, these studies simply correlate the decline of rainfall with senescence, but the lack of precipi-  
262 tation as a term in our best model suggests that other unmeasured factors are at play. Alternatively,  
263 **Zani2020** suggests that in resource limited environments, senescence times may largely be set by  
264 the preceding photosynthetic activity and sink-limitations on growth. For example, limited nutrient  
265 supply may prohibit photosynthesis late in the season if the preceding photosynthetic activity has  
266 depleted that supply. **Reich1992** suggested that there may be direct constraints on leaf life-span,  
267 especially in disturbance and drought-prone environments such as those studied here, which would  
268 lead to senescence rate being set largely by the time since bud-burst. In our study however, we  
269 found that there was variation in season length between plots, indicating that there are additional  
270 factors at play.

271 While leaf senescence is not as important for the survival of browsing herbivores as green-up, the  
272 timing of senescence with respect to temperature and precipitation has important consequences for  
273 the savanna understorey microclimate. The longer leaf material remains in the canopy after the  
274 end of the rainy season, the greater the microclimatic buffer for herbaceous understorey plants and  
275 animals, which require water and protection from high levels of insolation and dry air which can  
276 prevail rapidly after the end of the rainy season (). Our study merely exemplifies that more work  
277 needs to be done to properly characterise the drivers of senescence in this biome.

278 While species richness is a common measure of biodiversity, abundance evenness constitutes a second  
279 key axis (Wilsey et al., 2005; Hillebrand, Bennett, and Cadotte, 2008). While traditionally species

richness and evenness were assumed to be highly positively correlated, recent work has demonstrated that in many systems, richness and evenness may be nearly orthogonal (). In this study, we found contrasting effects of richness and evenness on both cumulative EVI and season length. Evenness caused a decrease in these phenological metrics, which we did not expect. It is possible that the negative effect of abundance evenness occurred because an increase in evenness is associated with a reduction in the canopy cover of a few highly dominant large canopy tree species (e.g. *Brachystegia boehmii* and *Julbernardia paniculata*), as part of the transition from woody savanna to thicket vegetation, or following a major disturbance event. Large canopy tree species have access to ground water for a longer part of the year, due to their deep root systems and conservative growth patterns. A future study may choose to explore the differential effects of species diversity in different size classes and in different physiognomic groups defined by functional form.

Our coverage of very short season lengths in Zambia, as estimated by the VIPPHEN product, was restricted, with notable absences of plot data in the northeast of the country around 30.5°E, 11.5°S, and 23.0°E, 15.0°S. Upon further inspection of true colour satellite imagery, these regions are largely seasonally water-logged floodplain and swampland, and were likely ignored by the ILUA-II assessment for this reason. This also explains their divergent phenological patterns.

It is important to note that the remotely sensed EVI measurements used here aren't specific only to trees, they represent the landscape as a single unit. Nevertheless, seasonal patterns of tree leaf phenology in southern African deciduous woodlands, particularly the pre-rainy season green-up phenomenon, is driven almost exclusively by trees, while grasses tend to follow patterns of precipitation more closely (). Grasses contribute to gross primary productivity, and it was therefore in our interests to include their response in our analysis as we seek to demonstrate how tree species richness can affect cycles of carbon exchange. Additionally, the micro-climatic effects of tree leaf canopy coverage and hydraulic lift through tree deep root systems will benefit the productivity of grasses as well as understorey tree individuals.

## 5 Conclusion

Here we explored the role of tree species diversity on land surface phenology across Zambia. We showed that species richness clearly affects rate of green-up, the lag time between rainy season onset and growth, and the length of the growing season. Our results have a range of consequences for earth system modellers and conservation managers, and lend further support to an already well established corpus of the positive effect of species diversity on ecosystem function.



## References

- Adole, Tracy, Jadunandan Dash, and Peter M. Atkinson (2018a). “Characterising the land surface phenology of Africa using 500 m MODIS EVI”. In: *Applied Geography* 90, pp. 187–199. DOI: 10.1016/j.apgeog.2017.12.006. URL: <https://doi.org/10.1016%2Fj.apgeog.2017.12.006>.
- (2018b). “Large-scale prerain vegetation green-up across Africa”. In: *Global Change Biology* 24.9, pp. 4054–4068. DOI: 10.1111/gcb.14310.
- Araujo, Helder F. P. de et al. (2017). “Passerine phenology in the largest tropical dry forest of South America: effects of climate and resource availability”. In: *Emu - Austral Ornithology* 117.1, pp. 78–91. DOI: 10.1080/01584197.2016.1265430.
- Bale, Jeffery S. et al. (2002). “Herbivory in global climate change research: direct effects of rising temperature on insect herbivores”. In: *Global Change Biology* 8.1, pp. 1–16. DOI: 10.1046/j.1365-2486.2002.00451.x.
- Chidumayo, E. N. (2001). “Climate and Phenology of Savanna Vegetation in Southern Africa”. In: *Journal of Vegetation Science* 12.3, p. 347. DOI: 10.2307/3236848.
- Cho, Moses A., Abel Ramoelo, and Luthando Dziba (2017). “Response of Land Surface Phenology to Variation in Tree Cover during Green-Up and Senescence Periods in the Semi-Arid Savanna of Southern Africa”. In: *Remote Sensing* 9.7, p. 689. DOI: 10.3390/rs9070689.
- Cole, Ella F., Peter R. Long, et al. (2015). “Predicting bird phenology from space: satellite-derived vegetation green-up signal uncovers spatial variation in phenological synchrony between birds and their environment”. In: *Ecology and Evolution* 5.21, pp. 5057–5074. DOI: 10.1002/ece3.1745.
- Cole, Ella F. and Ben C. Sheldon (2017). “The shifting phenological landscape: Within- and between-species variation in leaf emergence in a mixed-deciduous woodland”. In: *Ecology and Evolution* 7.4, pp. 1135–1147. DOI: 10.1002/ece3.2718.
- Didan, L. (2015). *MOD13Q1 MODIS/Terra Vegetation Indices 16-Day L3 Global 250m SIN Grid V006 [Data set]*. NASA EOSDIS Land Processes DAAC. DOI: 10.5067/MODIS/MOD13Q1.006. (Visited on 08/05/2020).
- Didan, L. and A. Barreto (2016). *NASA MEaSUREs Vegetation Index and Phenology (VIP) Phenology EVI2 Yearly Global 0.05Deg CMG [Data set]*. NASA EOSDIS Land Processes DAAC. DOI: 10.5067/MEaSUREs/VIP/VIPPHEN\_EVI2.004. (Visited on 08/05/2020).
- Dinerstein, Eric et al. (2017). “An Ecoregion-Based Approach to Protecting Half the Terrestrial Realm”. In: *BioScience* 67.6, pp. 534–545. DOI: 10.1093/biosci/bix014.
- Dray, Stéphane and Anne-Béatrice Dufour (2007). “The ade4 Package: Implementing the Duality Diagram for Ecologists”. In: *Journal of Statistical Software* 22.4, pp. 1–20. DOI: 10.18637/jss.v022.i04.

345 Dufrêne, M. and P. Legendre (1997). “Species assemblage and indicator species: the need for a  
 346 flexible asymmetrical approach”. In: *Ecological Monographs* 67, pp. 345–366. DOI: 10.1890/0012-  
 347 9615(1997)067[0345:SAAIST]2.0.CO;2.

348 Fayolle, Adeline et al. (2014). “Patterns of tree species composition across tropical African forests”.  
 349 In: *Journal of Biogeography* 41.12. Ed. by Peter Linder, pp. 2320–2331. DOI: 10.1111/jbi.12382.

350 Fenner, Michael (1998). “The phenology of growth and reproduction in plants”. In: *Perspectives in*  
 351 *Plant Ecology, Evolution and Systematics* 1.1, pp. 78–91. DOI: 10.1078/1433-8319-00053.

352 Fick, S. E. and R. J. Hijmans (2017). “WorldClim 2: New 1-km spatial resolution climate surfaces  
 353 for global land areas”. In: *International Journal of Climatology* 37.12, pp. 4302–4315. DOI: <http://dx.doi.org/10.1002/joc.5086>.

355 Fuller, Douglas O. (1999). “Canopy phenology of some mopane and miombo woodlands in eastern  
 356 Zambia”. In: *Global Ecology and Biogeography* 8.3-4, pp. 199–209. DOI: 10.1046/j.1365-2699.  
 357 1999.00130.x.

358 Gu, Lianhong et al. (2003). “Phenology of Vegetation Photosynthesis”. In: *Phenology: An Integrative*  
 359 *Environmental Science*. Springer Netherlands, pp. 467–485. DOI: 10.1007/978-94-007-0632-  
 360 3\_29.

361 Hillebrand, Helmut, Danuta M. Bennett, and Marc W. Cadotte (2008). “Consequences of dominance:  
 362 A review of evenness effects on local and regional ecosystem processes”. In: *Ecology* 89.6, pp. 1510–  
 363 1520. DOI: 10.1890/07-1053.1.

364 Huffman, G. J. et al. (2015). *GPM IMERG Final Precipitation L3 1 day 0.1 degree x 0.1 degree*  
 365 *V06 [Data set]*. Goddard Earth Sciences Data and Information Services Center (GES DISC). DOI:  
 366 10.5067/MODIS/MOD13Q1.006. (Visited on 10/30/2020).

367 Jeganathan, C., J. Dash, and P. M. Atkinson (2014). “Remotely sensed trends in the phenology  
 368 of northern high latitude terrestrial vegetation, controlling for land cover change and vegetation  
 369 type”. In: *Remote Sensing of Environment* 143, pp. 154–170. DOI: 10.1016/j.rse.2013.11.020.

370 Kreft, Holger and Walter Jetz (2010). “A framework for delineating biogeographical regions based on  
 371 species distributions”. In: *Journal of Biogeography* 37.11, pp. 2029–2053. DOI: 10.1111/j.1365-  
 372 2699.2010.02375.x.

373 Lüdtke, Daniel (2018). “ggeffects: Tidy Data Frames of Marginal Effects from Regression Models.”  
 374 In: *Journal of Open Source Software* 3.26, p. 772. DOI: 10.21105/joss.00772.

375 Medina, E. and M. Francisco (1994). “Photosynthesis and water relations of savanna tree species  
 376 differing in leaf phenology”. In: *Tree Physiology* 14.12, pp. 1367–1381. DOI: 10.1093/treephys/  
 377 14.12.1367.

378 Morellato, Leonor Patrícia Cerdeira et al. (2016). “Linking plant phenology to conservation biology”.  
 379 In: *Biological Conservation* 195, pp. 60–72. DOI: 10.1016/j.biocon.2015.12.033.

380 Mukosha, J and A Siampale (2009). *Integrated land use assessment Zambia 2005–2008*. Lusaka,  
381 Zambia: Ministry of Tourism, Environment et al.

382 Murtagh, Fionn and Pierre Legendre (2014). “Ward’s Hierarchical Agglomerative Clustering Method:  
383 Which Algorithms Implement Ward’s Criterion?” In: *Journal of Classification* 31.3, pp. 274–295.  
384 DOI: 10.1007/s00357-014-9161-z.

385 Ogutu, Joseph O., Hans-Peter Piepho, and Holly T. Dublin (2013). “Responses of phenology, syn-  
386 chrony and fecundity of breeding by African ungulates to interannual variation in rainfall”. In:  
387 *Wildlife Research* 40.8, p. 698. DOI: 10.1071/wr13117.

388 Parmesan, Camille (2007). “Influences of species, latitudes and methodologies on estimates of phe-  
389 nological response to global warming”. In: *Global Change Biology* 13.9, pp. 1860–1872. DOI: 10.  
390 1111/j.1365-2486.2007.01404.x.

391 Parr, C. L. et al. (2014). “Tropical grassy biomes: misunderstood, neglected, and under threat”. In:  
392 *Trends in Ecology and Evolution* 29, pp. 205–213. DOI: 10.1016/j.tree.2014.02.004.

393 Pelletier, J. et al. (2018). “Carbon sink despite large deforestation in African tropical dry forests  
394 (miombo woodlands)”. In: *Environmental Research Letters* 13, p. 094017. DOI: 10.1088/1748-  
395 9326/aadc9a.

396 Penuelas, J., T. Rutishauser, and I. Filella (2009). “Phenology Feedbacks on Climate Change”. In:  
397 *Science* 324.5929, pp. 887–888. DOI: 10.1126/science.1173004.

398 R Core Team (2020). *R: A Language and Environment for Statistical Computing*. R Foundation for  
399 Statistical Computing. Vienna, Austria. URL: <https://www.R-project.org/>.

400 Rousseeuw, Peter J. (1987). “Silhouettes: A graphical aid to the interpretation and validation of  
401 cluster analysis”. In: *Journal of Computational and Applied Mathematics* 20, pp. 53–65. DOI:  
402 10.1016/0377-0427(87)90125-7.

403 Smith, B. and J. B. Wilson (1996). “A consumer’s guide to evenness indices”. In: *Oikos* 76, pp. 70–82.  
404 DOI: 10.2307/3545749.

405 Stevens, Nicola et al. (2016). “Savanna woody encroachment is widespread across three continents”.  
406 In: *Global Change Biology* 23.1, pp. 235–244. DOI: 10.1111/gcb.13409.

407 White, Michael A. et al. (2009). “Intercomparison, interpretation, and assessment of spring phenology  
408 in North America estimated from remote sensing for 1982–2006”. In: *Global Change Biology* 15.10,  
409 pp. 2335–2359. DOI: 10.1111/j.1365-2486.2009.01910.x.

410 Wilsey, Brian J. et al. (2005). “Relationships among indices suggest that richness is an incomplete  
411 surrogate for grassland biodiversity”. In: *Ecology* 86.5, pp. 1178–1184. DOI: 10.1890/04-0394.

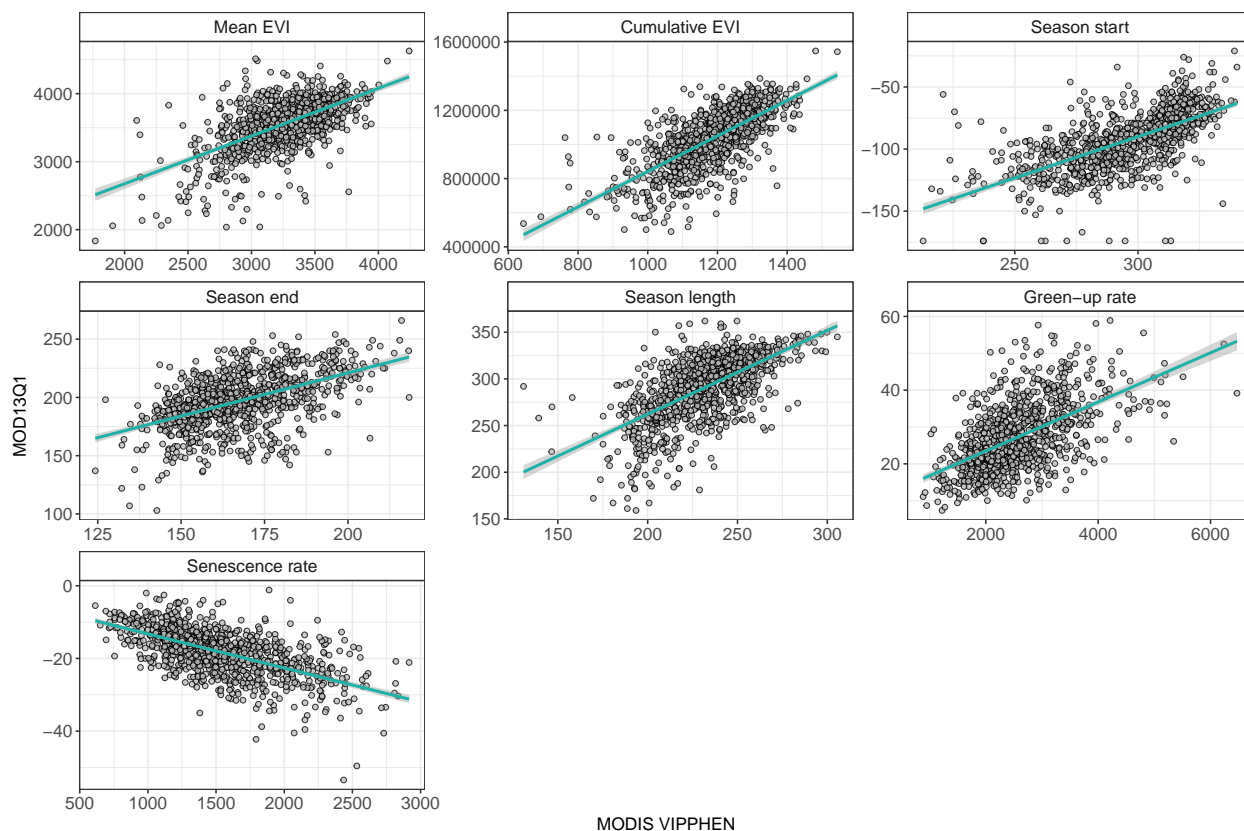


Figure S1: Scatter plots showing a comparison of phenological metrics from the MODIS VIPPHEN product (Didan and Barreto, 2016) and those extracted from the MOD13Q1 data (Didan, 2015), for each of the sites in our study. The cyan line shows a linear model of the data, with a 95% confidence interval.

Response	DoF	F	Prob.	R <sup>2</sup>
Mean EVI	960	521.3	p<0.05	0.35
Cumulative EVI	960	966.1	p<0.05	0.50
Season start	956	679.6	p<0.05	0.42
Season end	960	337.5	p<0.05	0.26
Season length	960	586.4	p<0.05	0.38
Green-up rate	960	432.4	p<0.05	0.31
Senescence rate	960	541.3	p<0.05	0.36

Table S1: Model fit statistics for comparison of MODIS VIPPHEN and MOD13Q1 products across each of our study sites.

Figure S2: Scatter plots showing pairwise comparisons of the six phenological metrics used in this study, extracted from the MODIS MOD13Q1 product (Didan, 2015). Points represent study sites and are coloured by vegetation type. Linear regression line of best fit for all sites is shown as a black line, while linear regressions are shown for each vegetation type cluster as coloured lines.

Rank	Precipitation	Diurnal dT	Evenness	Richness	Richness:Cluster	logLik	AIC	$\Delta IC$	$W_i$
1	✓	✓	✓	✓		<b>-9215</b>	<b>18445</b>	<b>0</b>	<b>0.749</b>
2	✓		✓	✓		-9218	18448	4	0.123
<u>3</u>	<u>✓</u>	<u>✓</u>	<u>✓</u>	<u>✓</u>	<u>✓</u>	<u>-9215</u>	<u>18449</u>	<u>4</u>	<u>0.106</u>
4	✓		✓	✓	✓	-9218	18452	7	0.022
5	✓	✓		✓		-9223	18459	14	0.001
6	✓			✓		-9227	18464	19	0.000
7	✓	✓				-9234	18478	34	0.000
8	✓	✓	✓			-9234	18480	35	0.000
9	✓	✓	✓		✓	-9233	18482	37	0.000
10	✓					-9237	18482	37	0.000

Table S2: Cumulative EVI model selection candidate models, with fit statistics. The overall best model is marked by bold text, while the best model with a richness:cluster interaction term is marked by underlined text

Rank	Precipitation	Diurnal dT	Evenness	Richness	Richness:Cluster	logLik	AIC	$\Delta IC$	$W_i$
1	✓	✓	✓	✓		-3322	6659	0	0.459
<b>2</b>	✓		✓	✓		<b>-3323</b>	<b>6659</b>	<b>0</b>	<b>0.405</b>
3	✓	✓	✓	✓	✓	-3322	6663	4	0.067
<u>4</u>	<u>✓</u>		<u>✓</u>	<u>✓</u>	<u>✓</u>	<u>-3323</u>	<u>6663</u>	<u>4</u>	<u>0.058</u>
5	✓			✓		-3329	6667	9	0.006
6	✓	✓		✓		-3328	6668	9	0.005
7	✓					-3334	6676	17	0.000
8	✓	✓				-3333	6676	17	0.000
9	✓	✓	✓			-3332	6677	18	0.000
10	✓		✓			-3334	6677	18	0.000

Table S3: Season length model selection candidate models, with fit statistics. The overall best model is marked by bold text, while the best model with a richness:cluster interaction term is marked by underlined text

Rank	Precipitation	Diurnal dT	Evenness	Richness	Richness:Cluster	logLik	AIC	$\Delta IC$	$W_i$
1	✓	✓	✓		✓	-2492	5000	0	0.282
<b>2</b>	✓	✓	✓			<b>-2494</b>	<b>5001</b>	<b>1</b>	<b>0.211</b>
3		✓	✓		✓	-2494	5002	1	0.146
4	✓	✓	✓	✓	✓	-2492	5002	2	0.119
5	✓	✓	✓	✓		-2494	5003	3	0.078
<u>6</u>		<u>✓</u>	<u>✓</u>			<u>-2497</u>	<u>5003</u>	<u>3</u>	<u>0.070</u>
7		✓	✓	✓	✓	-2494	5004	3	0.057
8		✓	✓	✓		-2497	5005	5	0.026
9	✓	✓		✓		-2498	5008	7	0.007
10	✓	✓				-2500	5009	9	0.004

Table S4: Green-up rate model selection candidate models, with fit statistics. The overall best model is marked by bold text, while the best model with a richness:cluster interaction term is marked by underlined text

Rank	Precipitation	Diurnal dT	Evenness	Richness	Richness:Cluster	logLik	AIC	$\Delta IC$	$W_i$
<u>1</u>	<u>✓</u>	<u>✓</u>	<u>✓</u>	<u>✓</u>		<b>-2248</b>	<b>4511</b>	<b>0</b>	<b>0.301</b>
2	✓	✓	✓	✓	✓	-2247	4512	1	0.169
3	✓		✓	✓		-2250	4512	2	0.131
4	✓	✓	✓			-2250	4513	2	0.098
5	✓		✓	✓	✓	-2249	4514	3	0.053
6	✓	✓	✓		✓	-2249	4514	3	0.053
7	✓		✓			-2252	4514	4	0.050
8	✓	✓				-2253	4515	4	0.034
9	✓					-2254	4515	5	0.029
10	✓		✓		✓	-2251	4516	5	0.024

Table S5: Senescence rate model selection candidate models, with fit statistics. The overall best model is marked by bold text, while the best model with a richness:cluster interaction term is marked by underlined text

Rank	Precipitation	Diurnal dT	Evenness	Richness	Richness:Cluster	logLik	AIC	$\Delta IC$	$W_i$
<b>1</b>	<b>✓</b>	<b>✓</b>	<b>✓</b>	<b>✓</b>		<b>-3030</b>	<b>6074</b>	<b>0</b>	<b>0.830</b>
2	✓	✓	✓	✓	✓	-3030	6077	3	0.170
<u>3</u>	<u>✓</u>	<u>✓</u>	<u>✓</u>		<u>✓</u>	<u>-3042</u>	<u>6100</u>	<u>26</u>	<u>0.000</u>
4	✓	✓	✓			-3045	6101	27	0.000
5	✓	✓				-3071	6152	78	0.000
6	✓		✓	✓	✓	-3069	6154	80	0.000
7	✓	✓		✓		-3071	6154	80	0.000
8		✓	✓	✓		-3071	6155	80	0.000
9	✓		✓	✓		-3072	6156	82	0.000
10		✓	✓	✓	✓	-3070	6157	82	0.000

Table S6: Green-up lag model selection candidate models, with fit statistics. The overall best model is marked by bold text, while the best model with a richness:cluster interaction term is marked by underlined text

Rank	Precipitation	Diurnal dT	Evenness	Richness	Richness:Cluster	logLik	AIC	$\Delta IC$	$W_i$
<b>1</b>	✓	✓	✓			<b>-3186</b>	<b>6385</b>	<b>0</b>	<b>0.182</b>
2		✓	✓	✓		-3186	6385	0	0.176
3		✓	✓			-3188	6385	0	0.168
4	✓	✓	✓	✓		-3186	6385	0	0.149
<u>5</u>		<u>✓</u>		<u>✓</u>		<u>-3188</u>	<u>6386</u>	<u>1</u>	<u>0.123</u>
6	✓	✓		✓		-3188	6387	2	0.058
7		✓	✓	✓	✓	-3186	6389	4	0.028
8	✓	✓	✓		✓	-3186	6389	4	0.027
9		✓	✓		✓	-3187	6389	4	0.025
10	✓	✓	✓	✓	✓	-3185	6389	4	0.024

Table S7: Senescence lag model selection candidate models, with fit statistics. The overall best model is marked by bold text, while the best model with a richness:cluster interaction term is marked by underlined text

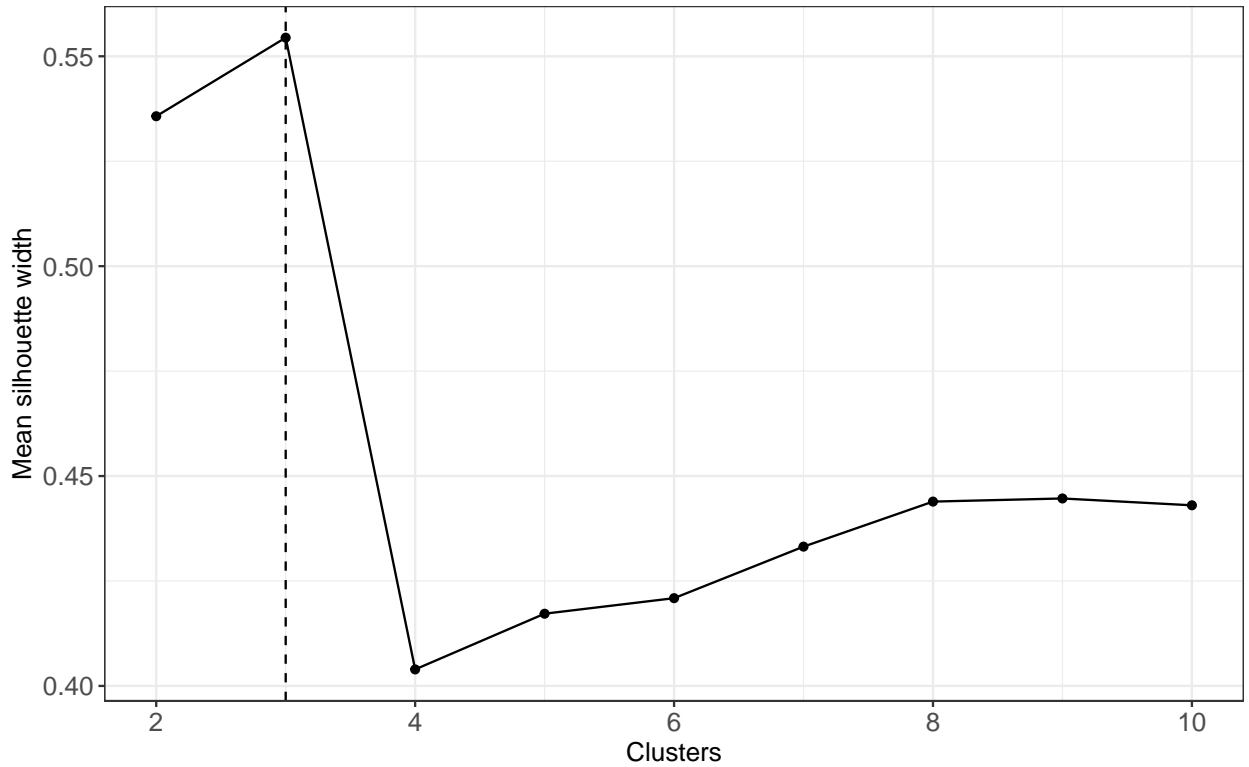


Figure S3: Mean silhouette width for agglomerative hierarchical clustering, specifying a varying number of clusters. The highest silhouette width, and therefore the number of clusters chosen in our analysis, is denoted by a dashed line.



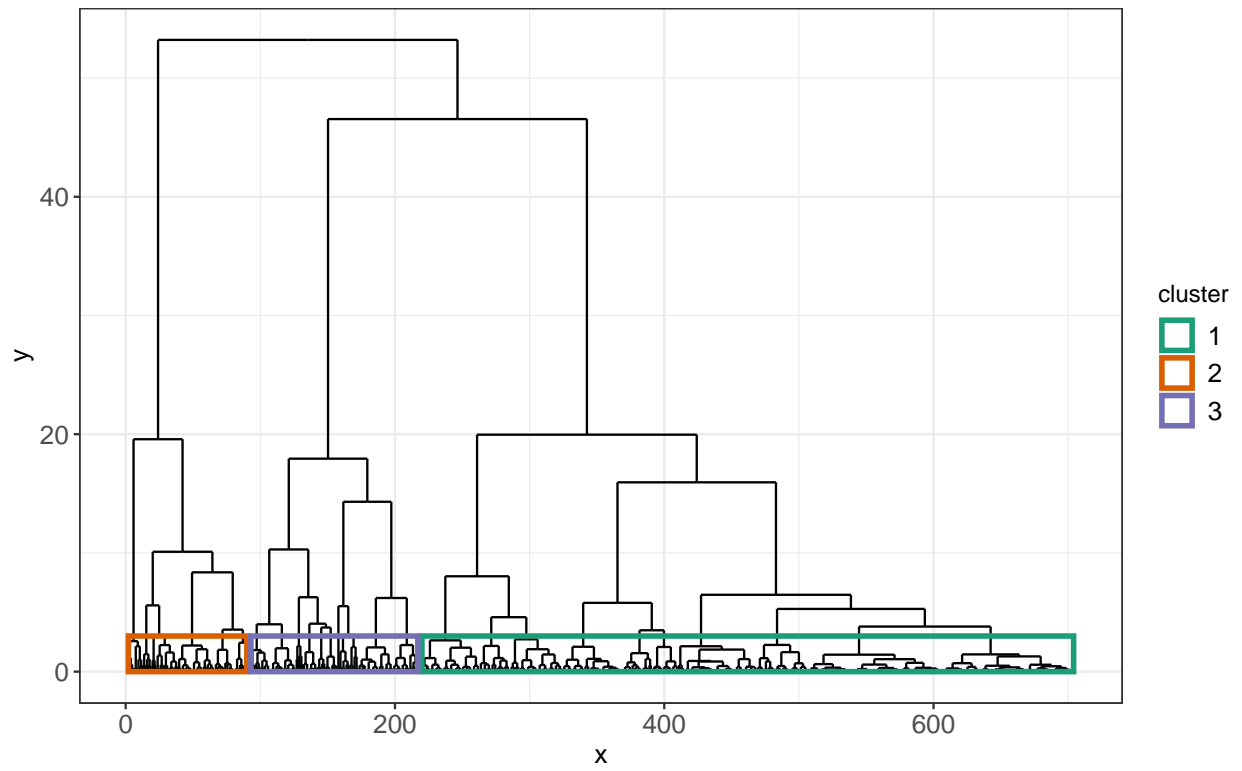


Figure S4: Dendrogram of hierarchical clustering of euclidean distances of NSCA (Non-Symmetric Correspondence Analysis) ordination axes, clustered using the Ward algorithm. Clusters are denoted by coloured boxes.

Response	Clusters	Estimate	SE	DoF	T ratio	Prob.
Cumulative EVI	1-2	1.1E-14	6.68E-14	697	0.17	0.98
	1-3	5.5E-14	6.33E-14	697	0.87	0.66
	2-3	4.4E-14	8.16E-14	697	0.54	0.85
Season length	1-2	-6.4E-18	1.56E-17	698	-0.41	0.91
	1-3	1.9E-17	1.48E-17	698	1.26	0.42
	2-3	2.5E-17	1.89E-17	698	1.32	0.38
Green-up rate	1-2	1.1E-18	4.89E-18	698	0.23	0.97
	1-3	-3.5E-18	4.59E-18	698	-0.76	0.73
	2-3	-4.6E-18	5.91E-18	698	-0.78	0.72
Senescence rate	1-2	3.7E-18	3.41E-18	698	1.09	0.52
	1-3	6.3E-18	3.21E-18	698	1.97	0.12
	2-3	2.6E-18	4.14E-18	698	0.63	0.80
Green-up lag	1-2	-7.3E-18	1.03E-17	698	-0.71	0.76
	1-3	6.0E-18	9.71E-18	698	0.62	0.81
	2-3	1.3E-17	1.25E-17	698	1.07	0.54
Senescence lag	1-2	2.9E-19	1.30E-17	698	0.02	1.00
	1-3	6.1E-18	1.23E-17	698	0.50	0.87
	2-3	5.9E-18	1.59E-17	698	0.37	0.93

Table S8: Comparisons of interaction marginal effects using post-hoc Tukey's tests.